JOURNAL OF OPTOELECTRONICS AND ADVANCED MATERIALS, Vol. 11, No. 6, June 2009, p. 797 - 812

Optical and photoelectric properties of GaSe, InSe - semiconductor oxide of In, Sn, Ti, Bi, Zn, Cu, Cd heterojunctions

IG. EVTODIEV[a], IU. CARAMAN[c], D. DAVIDESCU[b], A. DAFINEI[b*],
V. NEDEFF[c], M. CARAMAN[c], E. CUCULESCU[a]
[a]*Moldova State University, 60 A. Mateevici Str., Chisinau, MD-2009, Republic of Moldova*
[b]*University of Bucharest, Bucharest - Magurele, CP MG-11, RO 077125 Bucharest, Romania*
[c]*University of Bacau, 157 Calea Marasesti, R-600115 Bacau, Romania*

This paper examines the influence of constituent materials properties on the optical and photoelectrical characteristics of the heterojunctions. The edge of intrinsic absorption band of GaSe and InSe crystals, at the temperature of 78 K, consists of direct exciton bands from the states n=1 and n=2. Effective mass electron-hole pair in InSe is equal to 0.14 m_0. Effective mass of electrons in *p-GaSe* is equal to 0.18 m_0. Oxide-GaSe and oxide-GaSe heterojunctions were manufactured by thermal oxidation of In*, Sn, Ti, Bi, Zn, Cu* and Cd metallic films. The heterojunctions of GaSe and InSe semiconductors with studied oxides of metals reveal high photosensitivity in the visible and near IR spectrum. Photosensitivity band edge to low energies is determined by the GaSe or InSe band gap and the edge to high energy edge - by the respective oxides' gap. Free path of minority charge carriers in GaSe layer at the TiO_2/GaSe:Cu, In_2O_3/InSe and TiO_2/InSe heterojunction's interface depends on the fabrication technology and ranges between 0.56 μm÷1.97μm. The same parameter for structures based on InSe lies between 1,00÷3,45 μm for structures based on p-GaSe.

(Received April 5, 2009; after revision June 6, 2009; accepted June 15, 2009)

Keywords: GaSe, InSe, transparent metal oxide, exciton, light absorption, photoelectric properties of heterojunctions.Introduction

$GaSe$ and $InSe$ are representatives of a wide class of semiconductor materials with stratified crystalline structure [1, 2]. In these crystals the forces linking the atoms inside of layered packaging are strong (due to the pairs of electrons) while the bonds between packing are weaker, Van der Waals forces.

The specific arrangement of atomic planes in order Chalcogen-Metal-Metal-Chalcogen results in valence bonds of the wrapping surfaces are mostly closed resulting in a low concentration of surface states [3] [4] . This property, and the band gap value of $2.0eV$ for $GaSe$ and of $1.26eV$ for $InSe$ [5] , [6] ranks these materials among semiconductors with various applications in optoelectronics and especially as detectors of radiation with wide technical use [7] , [8] and photovoltaic cells [9] , [10] .

Photoelectrical properties of $pGaSe-nInSe$ heterojunctions with optical transparent contact [11-13] and with optical transparent semiconductors In_2O_3 (SnO_2) [14] [15] [16] are quite well studied. The spectral characteristics of photosensitivity are dependent on the technology of oxide manufacturing. The Indium Oxide used in In_2O_3-InSe heterojunctions studied in [15] , [16] are obtained by thermal oxidation or by prolonged oxidation at normal temperature in air. It was established that with increasing oxidation time the edge of spectral characteristics shifts from high energy to lower energies.

Thus photosensitivity range covers the energies from $1.20eV$ up to $\sim 2.1eV$, although In_2O_3 layer is optically transparent up to $\sim 4.0eV$. During the thermal oxidation on the surface film of $InSe$ a nano-defects ordered system is formed. It influences the mechanism of charge separation in the junction and causes the photosensitivity increases in the range of excitonic absorption band [17] .

The paper reports results of the investigation of the optical properties of $InSe$ and $GaSe:Cu$ crystals used as basic element of heterojunctions and of Zn , Cd , Cu , In , Bi and Sn , semiconductor oxides. The studies on photoelectrical properties and some questions on charge transport mechanisms in heterojunctions are also discussed.

1. General concepts

When the surface of a semiconductor is illuminated with monochromatic light having the energy $E_f = h\nu$, part of this is absorbed in the material having the absorption coefficient $\alpha(h\nu)$ and other part is reflected. Photoelectrical effects are determined by light absorption mechanisms. The spectral distribution of relative absorption coefficient of a semiconductor is shown

schematically in Figure 1. The photons absorbed in the first spectral domain cause the generation of non-equilibrium charge carriers (electrons or holes), which in results in electrical conductivity $\sigma(h\nu)$ increase, while a generation of hole-electron pairs can be produced only through band-to-band, absorption when the condition $h\nu \geq E_g$ is satisfied.

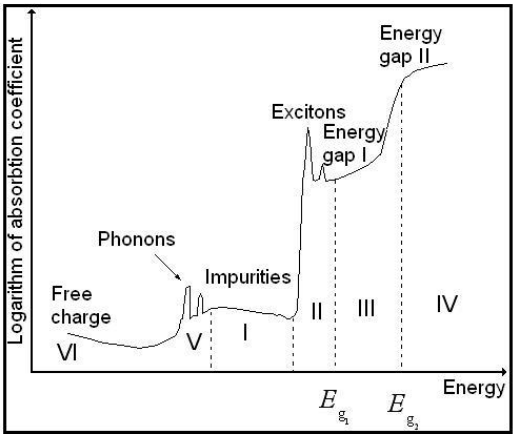

Fig. 1. The spectral distribution of relative absorption coefficient for semiconductors.

A pronounced increase of photosensitivity takes place for energies $h\nu \geq E_{g_2}$, when in generation process of electron-hole pairs are also included transitions of the electrons from the second valence sub-band (Region IV). At low temperatures under the influence of electromagnetic radiation in the spectral range VI the mobility of free charge carriers may change, which under certain conditions will lead to the variation in electrical conductivity of the material. Corresponding photoconductivity band has not a low photon energy edge [18] .

Along with the generation of electron-hole pairs with generating rate „ g ”, a recombination process having rate „ r_n ” and „ r_p ” (for electrons and holes respectively) takes place.

In Figure 2 are illustrated electronic transitions for a system with three energy levels.

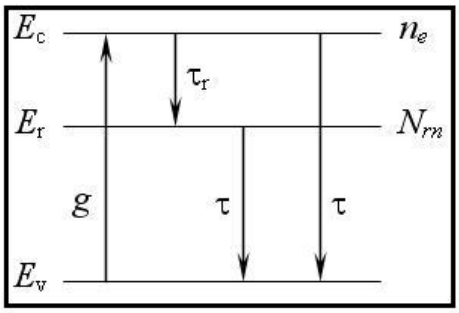

Fig. 2. The system with three energylevels; the generation and recombination of non-equilibrium electrons.

The concentration of excess electrons and holes at any moment of time is equal to the difference between photo-generation and recombination rates:

$$\frac{\partial n}{\partial t} = g_n - r_n \quad ; \quad \frac{\partial p}{\partial t} = g_p - r_p . \tag{1}$$

The generation of the charge carriers includes the thermal generation of electrons (characterized by g_{0n}) and holes g_{0p} and also optical generation g_F. For band to band absorption, the rate of photo-generation for electron and holes are equal ($g_{Fn} = g_{Fp} = g_F$).

If N_f is the number of incident photons on the sample surface for 1 sec, then the photo-generation rate is given by:

$$g_F = \alpha N_f (1-R)\eta \tag{2}$$

where R is the reflection coefficient, α is the absorption coefficient and η is the quantum yield at a given photon energy.

The rate of recombination for band to band electron transitions is directly proportional to the concentration of charge carriers $\Delta n = \Delta p$ and to concentration of recombination centers for electrons and holes:

$$r_n = \gamma_n n N_{r_n} = \frac{n}{\tau_n}, \quad r_p = \gamma_p p N_{r_p} = \frac{p}{\tau_p} \tag{3}$$

where γ_n and γ_p are recombination coefficients for electrons and holes and τ_n and τ_p are mean life time for electrons and holes respectively.

Reflection coefficient R for the non-polarized incident light is written as:

$$R = \frac{1}{2}\left(R_s + R_p\right) \tag{4}$$

where R_s and R_p are coefficients of reflection for light polarized perpendicular and respectively parallel to the plane of incidence.

At normal incidence in air $(n_0 = 1)$ [19] T. S. [20] :

$$R = R_s = R_p = \frac{(n-1)^2 + k^2}{(n+1)^2 + k^2} . \tag{5}$$

Due to the fact that oxide semiconductors (TiO_2, In_2O_3, SnO_2, ZnO, Bi_2O_3) are optically transparent ($k \cong 0$) for spectral range $\lambda > 400nm$, the reflection coefficient of (2) can be determined from measurements of refractive index " n ".

The process of optical generation of charge carriers can result in formation of an electromotive force, if some

requirements are satisfied. The formation of a gradient of charge carriers so that both electrons and holes move through the sample, by diffusion, independent from each other is one of the possible requirements.

The density of electric current through the semiconductor junction (Figure 3) is determined by the diffusion of minority charge carriers [21] and is given by the expression:

$$i_p = -\frac{e(1-R)\alpha \cdot L_p \cdot N_f \cdot \exp(-\alpha d_n)}{1+\alpha \cdot L_p} + \\ + \frac{eD_p p_{n0}}{L_p}\left[\exp\left(\frac{qV}{kT}\right)-1\right] \quad (6)$$

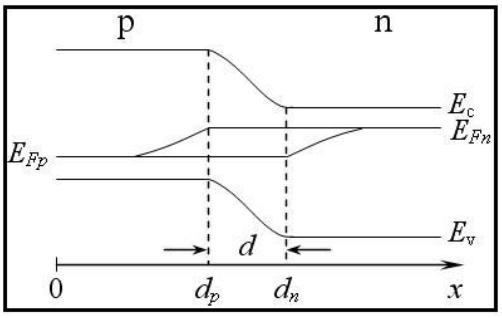

Fig. 3. The diagram of energetic levels in biased p-n junction.

Also, under the open circuit, the voltage in photovoltaic junction is given by the expression [22] :

$$V = -\frac{kT}{e}\ln\left(1+\frac{(1-R)N_f\left[1-\left(e^{-\alpha d_n}\right)/\left(\alpha L_p+1\right)\right]}{\frac{D_p p_{n0}}{L_p}+N_c\left(v_n+S_n\right)e^{-e\cdot(V_D/kT)}}\right) \quad (7)$$

where L_p is free path and D_p is diffusion coefficient of holes; V_D - biasing voltage at the junction; S_n - the recombination rate of electrons at the separation surface between optically transparent electrode and semiconductor; v_n - thermal speed of electrons.

The efficiency η of photo-voltaic cells depends both on the mechanism of generation-recombination and transport of the non-equilibrium charge carriers (internal efficiency), and spectral distribution of energy emitted by radiation source (external efficiency). Maximal yield of the cell $\eta_{\max}$ determined as the ratio of the maximum electrical power generated by the cell by incident light energy is given by the expression [23] :

$$\eta_{\max} = \frac{e^2(1-R)\cdot\left(1-e^{-\alpha d}\right)V_m^2 n_f}{\left(kT+eV_m\right)N_f E_A} \quad (8)$$

where V_m is the open circuit voltage, E_A - average energy for the absorbed photons beam in the active part of junction, N_f is the density of photon beam having the energy $h\nu \geq E_g$ which creates electron-hole pairs in junction; N_f depends on the correlation between spectral energy distribution of light source and the rate of generation of electron-hole pairs.

2. Experimental results

The spectral distribution (in relative units) of density of solar radiation outside the atmosphere (curve 1) [24] , at the land surface (curve 2) [25] and spectral distribution of photocurrent (normalized to unity) in $GaSe$, $GaTe$, $InSe$ and $CdTe$ semiconductors, (curves 3-6, respectively) are presented in Figure 4. Low density of surface states, as well as good correlation between solar radiation spectrum and spectral characteristics of photocurrent, allows to associate $InSe$ and $GaTe$ layered compounds to the class of semiconductor materials useful for the manufacturing of semiconductor solar cells with optimal efficiency.

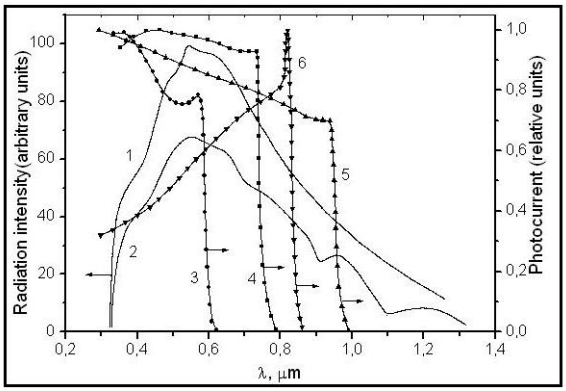

Fig. 4. Spectral distribution (in relative units) for density of solar radiation outside the atmosphere (curve 1), at the land surface (curve 2) [26] and spectral distribution of photocurrent relative to the number of photons absorbed and normalized to unity in semiconductors GaSe (curve 3), GaTe (curve 4), InSe (curve 5) and CdTe (curve 6).

GaSe

The absorption spectra $\alpha(h\nu)$ of $GaSe$ at $293K$ and $78K$ are presented in Figure 5. At the fundamental absorption band edge, at $293K$ (curve 1), the plot shows an exciton absorption narrow band with a maximum at $2.00eV$. The maximum value for coefficient of absorption in this band is $\sim 1700\,cm^{-1}$. The decrease of the sample temperature to $78K$ (curve 2) results in the excitonic band width monotonically decrease. The coefficient of absorption in center of band increases up to

$\sim 2000\,cm^{-1}$. Also, the band is shifted towards high energies. Temperature dependence of excitonic energy maximum is given by polynomial [27] Y. P. :

$$E_{exc}(T) = E_{exc}(0) - \frac{\alpha T^2}{T+\beta}, \tag{9}$$

were energy of exciton at $0K$ absolute temperature is $E_{ex}(0) = 2.134eV$, thermal coefficient $\alpha = 2.33\times10^{-4} eV/K$ [28] and $\beta = -38.5K$.

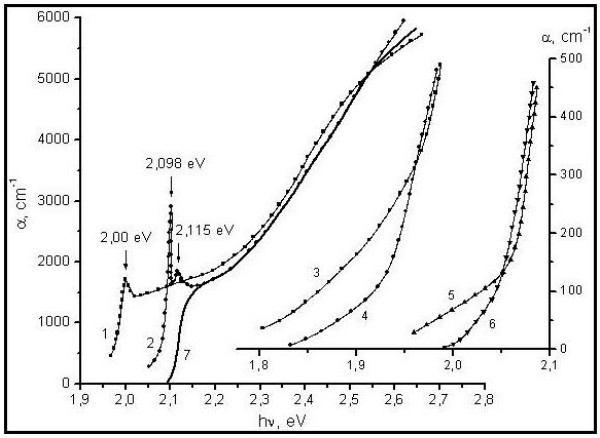

Fig. 5. Absorption spectra of $GaSe$ crystal for room temperature $293K$ (curves 1, 3, 4) and for liquid nitrogen $78K$ (curves 2, 5, 6) in polarization $\vec{E}\,\|\,\vec{C}$ (curves 3, 5) and $\vec{E}\perp\vec{C}$ (curves 1, 2, 4, 6). Curve 7 was calculated by use of formula (12) for $\alpha_0 = 1630\,cm^{-1}$ at $h\nu = 2.175eV$.

At low temperatures ($T = 78K$), together with the line corresponding to the excitonic state $n=1$ ($E_{n=1} = 2.098eV$), the absorption band corresponding to the excitonic state $n=2$ appears at $E_{n=2} = 2.115eV$.

If the electron energy is determined from the valence band top, then in the first approximation, the energy required to form excitonic band in the center of Brillouin zone ($k=0$) $E_n(0)$ is given by the formula [29] :

$$E_n(0) = E_g - R/n^2, \tag{10}$$

where E_g is the band gap, $n = 1,2,3,\ldots$ - main quantum number, R - effective excitonic Rydberg constant. Using values of excitonic energy bands for $n=1$ and $n=2$ one can determine the band gap at $78K$ - $E_g = 2.121eV$ and the value of excitonic Rydberg, $R = 22.6eV$.

For three-dimensional excitons, the energy related to electron-hole pair is determined from the dependence [30] :

$$R = 1{,}360\,\frac{\mu}{\varepsilon^2}\text{, eV} \tag{11}$$

where $\mu = \left(m_n^{-1} + m_p^{-1}\right)^{-1}$ is the reduced mass of electron-hole pair, and ε - for anisotropic crystals as $GaSe$ - is calculated from [31] M. S. $\varepsilon = \left(\varepsilon^{II}\cdot\left(\varepsilon^{\perp}\right)^2\right)^{1/3}$. Considering that $m_p = 0.55m_0$ [32], $\varepsilon_0^{\perp} = 10.2$ and $\varepsilon_0^{II} = 7.6$ [31] M. S. the effective mass of minority charge carriers is $m_n = 0.18m_0$. This value correlates well with results of magneto-optical measurements [32].

In addition to the spectrum with excitonic lines at discrete energies $h\nu > E_g$, one may observe the so-called excitonic continuum, where overlapping lines with $n > 2$. In this spectral range the absorption coefficient $\alpha(h\nu)$ for direct optical transitions is given by the formula [33] [34] :

$$\alpha(h\nu) = \frac{\alpha_0(h\nu)\pi\gamma\exp(\pi\gamma)}{sh(\pi\gamma)} \tag{12}$$

where $\alpha_0(h\nu)$ is the absorption coefficient for $h\nu >> E_g$, in this energy range the electrons and the holes do not interact; $\gamma^2 = R/(h\nu - E_g)$.

In Figure 5 (curve 7) is shown the dependence $\alpha(h\nu)$ calculated by use of formula (12) for $\alpha_0 = 1630\,cm^{-1}$ at $h\nu = 2.175eV$.

Deep inside the fundamental band, absorption coefficient increases monotonically with energy increase, both at room temperature and at $78K$, reaching the value of $\sim 5200\,cm^{-1}$ at $h\nu = 2.55eV$.

Due to their layered structure, $GaSe$ crystals show a strong anisotropy of mechanical properties, which manifests themselves in electrical and optical properties (refractive indexes and absorption coefficients in a wide range of energy receiving different values as function of polarization $\vec{E}\,\|\,\vec{C}$ and $\vec{E}\perp\vec{C}$) [35] [36] . As can be seen from Figure 5 (curves 3-6), anisotropic optical absorption is pronounced in the optical transitions region with the formation of indirect excitons ($E_{exc}^{i} = 2.050eV$, $T = 80K$ [37]). In this range of energy absorption coefficient is less than $300\,cm^{-1}$ at $T = 293K$ and $\sim 130\,cm^{-1}$ at $78K$ and decrease monotonically with energy. Also, in this energy range, the absorption of light in both $\vec{E}\,\|\,\vec{C}$ and $\vec{E}\perp\vec{C}$ polarization is characterized with the absorption coefficients $\alpha_{II} > \alpha_{\perp}$. This leads to the conclusion that at $T \geq 78K$ in $GaSe$ the lowest

energy state is the state of indirect excitons, in which optical transitions are allowed for $\vec{E} \parallel \vec{C}$ polarization and only partly for $\vec{E} \perp \vec{C}$ polarization.

InSe

The light absorption at the edge and deep inside of fundamental absorption band for mono crystalline layers of $InSe$ ($0.02\% at.Cu$) at $78K$ and $293K$ was investigated.

Absorption spectra in the range of $1.05eV$ - $2.65eV$ are shown in Figure 6. The absorption band edge of the $InSe$ crystal ($0.02\% at.Cu$) at $T = 293K$ (curve 1) shows a peak at $1.265eV$. At lower temperatures, the absorption band edge is amplified and it shifts monotonically toward higher energy, along with its width decrease. Dependence of excitonic energy band on temperature satisfies the formula (9) in which $E_{exc}(0) = 1.332eV$, $\alpha = 4.70 \times 10^{-4} eV/K$ and $\beta = 233K$.

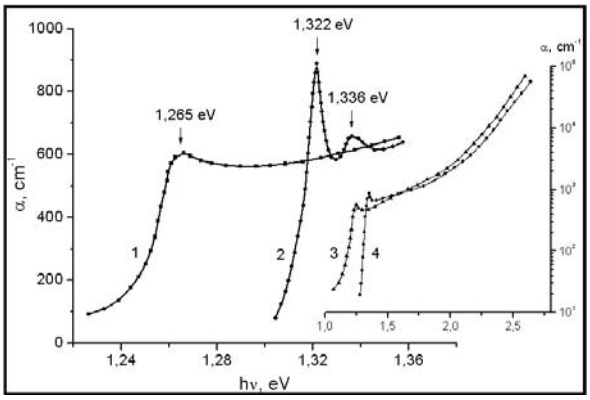

Fig. 6. Absorption spectra of monocrystalline layers of $InSe$ ($0.02\% at.Cu$) at a temperature of $293K$ (curve 1, 3) and $78K$ (curve 2, 4).

At $78K$ the edge of absorption band is formed of two bands corresponding to direct excitons in the $n = 1$ ($h\nu = 1.322eV$) and $n = 2$ ($h\nu = 1.336eV$) states. Using the energy of electron-hole pairs (exciton) from (10), one obtain $R = 18.7meV$.

Also, as it comes from (11), and taking into account that $\varepsilon_0^{\perp} = 10.9$, $\varepsilon_0^{\parallel} = 9.9$ [38] Physical and chemical properties of semiconductors – Z. S. Medvedeva, O. N. Kalashnik, Ia. A. Kalashnikov, - Moskva, Nauka, 1979, - p 339 (in Russian)., it was determined that $\varepsilon_0 = 10.7$ and reduced mass of electron-hole pair as being equal to $\mu = 0.14m_0$, where m_0 is the mass of free electron.

As one can see in the inset to Figure 6, the absorption coefficient $\alpha(h\nu)$ at higher energies at $293K$ (curve 3) and $78K$ (curve 4) increases monotonically with energy, reaching the value of $\sim 7 \times 10^5 cm^{-1}$ at $2.6eV$.

In_2O_3

In_2O_3 thin layers obtained on a substrate of SiO_2 by heat treatment at temperature $T = 670K$ in the air of an In layer having the thicknesses in the range of $0.11\mu m$ - $2.3\mu m$ have been investigated. The treatment time was $15, 20$ and 35 minutes and it was selected for the optical transmission at $632.8nm$ to exceed 70%. In Figure 7 the absorption spectra of thin layers of In_2O_3 at the temperature $293K$ are presented. The $\alpha(h\nu)$ dependencies for air heat-treated layers at different time have similar shapes and contain three distinct intervals. In the energies range $1.5eV \le h\nu \le 2.7eV$ absorption coefficient has a weak dependence on photons' energy and weakly decreases with increasing of treatment time from $3000cm^{-1}$ ($t = 15\min$) down to $\sim 760cm^{-1}$ ($t = 35\min$) (wavelength of the light-probe $\lambda = 632.8nm$).

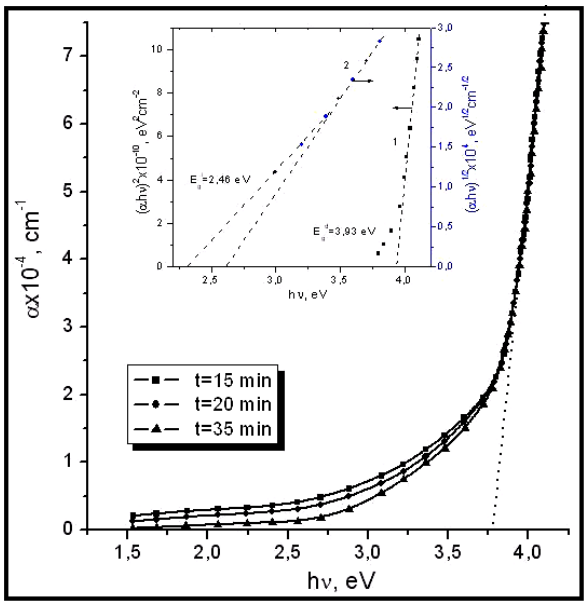

Fig. 7. Absorption spectra of thin layers of In_2O_3 at temperature $293K$ heat-treated for $15,20$ and 35 minutes. Inset: dependence $(\alpha h\nu)^{1/2} = f(h\nu)$ (curve 1) and $(\alpha h\nu)^2 = f(h\nu)$ (curve 2) for thin layers of In_2O_3 at temperature $293K$.

In the range of $2.7eV \le h\nu \ge 3.7eV$ the absorption coefficient monotonically increases up to $\sim 1.8\times10^4\, cm^{-1}$ and shows a steep increase for $h\nu > 3.7eV$. By extrapolation of the steep increase segment of the absorption coefficient to $\alpha = 0$ one approximates the optical band gap for In_2O_3 layers - $E_g^0 = 3.8eV$. In this energy range, the dependence $\alpha(h\nu)$ is well described by a power function of the type:

$$\alpha(h\nu) = A(h\nu - E_g)^n \qquad (13)$$

Power factor $n = 1/2$ for $h\nu > 3.9eV$, corresponds to direct optical transitions (valence band - conduction band) (inset to Figure 6, curve 2). Band gap, determined by extrapolation of linear dependence segment $(\alpha h\nu)^2 = f(h\nu)$ to $\alpha = 0$ is equal to $3.93eV$. It has been demonstrated [39] that direct optical band gap depends on the thickness of layers obtained on a glass support and varies within $(3.0 \div 3.6)eV$.

In the $(2.5 \div 3.8)eV$ range, the power factor (13) is equal to $n = 2$, which corresponds to indirect optical transitions [49] . Indirect band gap E_g^i at $293\,K$ was determined by extrapolation of $(\alpha h\nu)^{1/2} = f(h\nu)$ to $\alpha = 0$ equals to $2.46eV$.

SnO_2

SnO_2 part of $SnO_2/p-GaSe(Cu)$ and $SnO_2/p-InSe(Cu)$ heterojunctions were obtained by heat treatment of thin layers of Sn at $520\,K$ in air. SnO_2 has been also obtained on amorphous SiO_2 substrate. The absorption spectra at $T = 293\,K$ of the layers of SnO_2 with thickness of $0.15\,nm$ up to $2.8\ nm$ are given in Fig. 8.

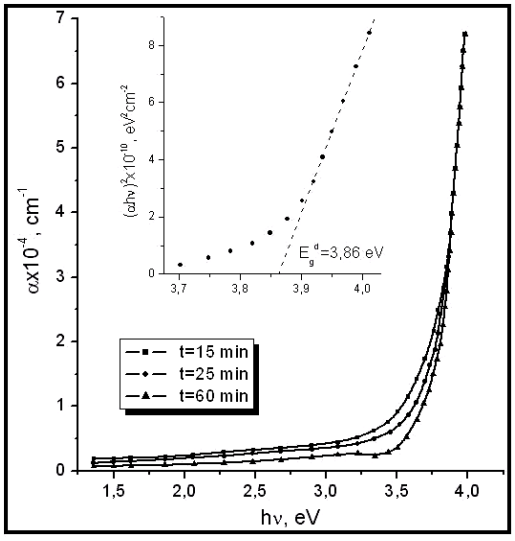

Fig. 8. Absorption spectra at temperature of 293 K of thin layers of SnO_2 heat-treated for 15,25 and 60 min.. Inset: dependence $(\alpha h\nu)^2 = f(h\nu)$ of thin layers of SnO_2 at 293 K.

As can be seen in the $1.35eV$ - $3.2eV$ range, the absorption coefficient increases monotonically with energy from $\sim 800\,cm^{-1}$ up to $\sim 2200\,cm^{-1}$ (SnO_2 layers were oxidized for $60\,\text{min}$).

The slow increase of the absorption coefficient with energy characteristic is kept for SnO_2 layers obtained by oxidation of Sn layer for $15\,\text{min}$ and $25\,\text{min}$ as well.

At $h\nu > 3.7eV$ the absorption coefficient increases sharply reaching the value of $7\times10^4\,cm^{-1}$ at $4.0eV$. In this range, as it can be seen from the inset to Figure 8, direct optical transitions occurs. The band gap corresponding to direct optical transitions is equal to $3.86eV$ and does not depend on the oxidation time for Sn layer on the SiO_2 substrate.

TiO_2

In Fig. 9, the absorption spectra at $293\,K$ for the TiO_2 layers produced by reactive evaporation in $Ar:O_2$ plasma $(75:25)$ in DC current with the density of $2.5\,mA/cm^2$ up to $12\,mA/cm^2$ are shown. As source, a disk of $Ti(96\%)$ was used. The thickness of the layers studied varied in the range of $(120 \div 350)nm$. As can be seen from the comparison of curves 1-4 (Figure 9), the titanium oxide layers are optically transparent in the range of energies from $1.35eV$ up to $\sim 2.8eV$. The coefficient of absorption in this energy range depends on density of current of evaporation and is increasing with the density of current in plasma.

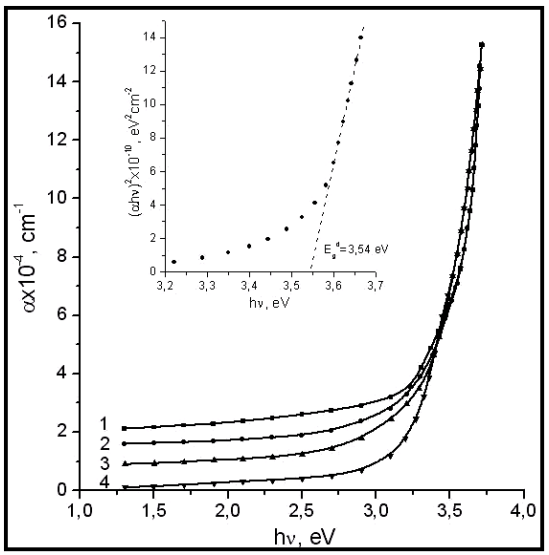

Fig. 9. Absorption spectra of the layers of TiO_2 at a temperature of 293 K. Density of evaporation current: $12\,mA/cm^2$ (curve 1), $7.5\,mA/cm^2$ (curve 2), $5\,mA/cm^2$ (curve 3) and $2.5\,mA/cm^2$ (curve 4). Inset: dependence $(\alpha h\nu)^2 = f(h\nu)$ of the layers of TiO_2 at 293 K.

At $\lambda = 632.8 nm$, the absorption coefficient is $3.3\times10^3 cm^{-1}$, $1.1\times10^4 cm^{-1}$, $1.7\times10^4 cm^{-1}$ and $2.3\times10^4 cm^{-1}$ for the current density of $2.5 mA/cm^2$, $5 mA/cm^2$, $7.5 mA/cm^2$ and $12 mA/cm^2$, respectively.

For $h\nu > 3.5 eV$ one can observe a steep increase of absorption coefficient with energy. In this spectral range, the $\alpha(h\nu)$ plots for the investigated samples, practically coincide and satisfy the requirement for direct optical transitions. At the band gap at $T = 293 K$ of the titanium oxide layers, determined by extrapolation of segment of linear dependence $(\alpha h\nu)^2 = f(h\nu)$ is equal to $3.54 eV$. Using reactive evaporation method in the presence of plasma $Ar:O_2$ were obtained TiO_2 thin layers [41] in which occurs optical direct transitions; forbidden band width of TiO_2 layers is equal to $3.6 eV$ at $293 K$.

Bi_2O_3

Thin layers of Bi_2O_3, part of heterojunctions $Bi_2O_3/GaSe$ and $Bi_2O_3/InSe$ were obtained by reactive evaporation in $Ar:O_2$ plasma ($75:25$) in DC.

Current density was $250 \mu A/cm^2$, $620 \mu A/cm^2$ and $1200 \mu A/cm^2$. In the same technological conditions Bi_2O_3 - thin layers on support of amorphous SiO_2, used for optical studies at the temperature of $293 K$ have been prepared. The thicknesses of investigated samples was from $0.13 \mu m$ up to $1.8 \mu m$.

In Fig. 10 the absorption spectra of Bi_2O_3 layers in the energy range from $1.4 eV$ up to $4.0 eV$ are presented.

As can be seen from these graphs, the $\alpha(h\nu)$ spectral dependency for $h\nu < 3.65 eV$ depends on current density in $Ar:O_2$ plasma. In the range of $(1.35 eV \le h\nu \le 3.7 eV)$ the absorption coefficient is increasing with current density. $\alpha(h\nu)$ coincides only for $h\nu > 3.75 eV$ where $\alpha > 4.3\times10^4 cm^{-1}$. In this energy range, the $(\alpha h\nu)^2 = f(h\nu)$ plot is a segment. Its extrapolation to $\alpha = 0$ gives the direct band gap equal to $3.9 eV$ (Figure 10, inset, curve 1).

In the range of $h\nu < 3.7 eV$ the absorption spectra are well described by a power function (13) where $n = 1/2$. The dependence $(\alpha h\nu)^{1/2} = f(h\nu)$ for Bi_2O_3 layers obtained at current density of $620 \mu A/cm^2$ in $Ar:O_2$.

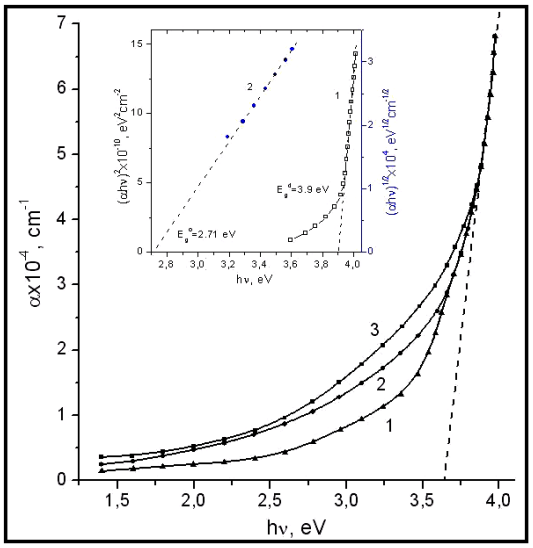

Fig. 10. Absorption spectra of Bi_2O_3 layers at $293 K$. The current density: $250 \mu A/cm^2$ (curve 1), $620 \mu A/cm^2$ (curve 2) and $1200 \mu A/cm^2$ (curve 3). Inset: $(\alpha h\nu)^2 = f(h\nu)$ dependence (curve 1) and $(\alpha h\nu)^{1/2} = f(h\nu)$ (curve 2) of the layers of Bi_2O_3 (current density $620 \mu A/cm^2$.

Optical band gap determined by extrapolation of the linear segment $(\alpha h\nu)^{1/2} = f(h\nu)$ to $\alpha h\nu = 0$, is equal to $2.71 eV$.

ZnO

The absorption spectra at $T = 293 K$, of ZnO thin layers obtained by reactive evaporation method in $Ar:O_2$ ($75:25$) atmosphere using DC current on amorphous SiO_2 support are shown in Figure 11. The current densities were $250 \mu A/cm^2$, $620 \mu A/cm^2$ and $1.2 mA/cm^2$. The edge of intrinsic absorption band is localized at $h\nu > 3.7 eV$. In this energy range, the $\alpha(h\nu)$ plot for ZnO layers, at a current density of $(0.25 \div 1.2) mA/cm^2$ practically coincide (Figure 11).

In the inset in Figure 11 the dependence $(\alpha h\nu)^2 = f(h\nu)$ for ZnO layers with thicknesses in the range of $(120 \div 2300) nm$, obtained at current density of $620 \mu A/cm^2$ in $Ar:O_2$ plasma is presented. This energy dependence in $3.9 eV < h\nu < 4.2 eV$ energy range is a straight segment corresponding to the direct optical transitions. The width of direct band gap equals to $E_g^d = 3.89 eV$.

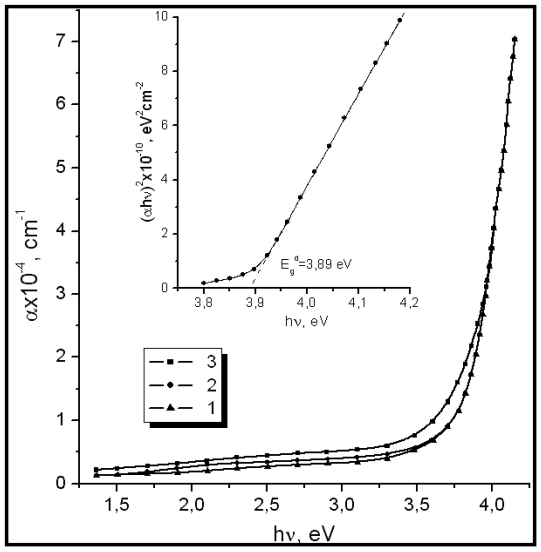

Fig. 11. Absorption spectra of ZnO *thin layers at the* $293\,K$. *The current density current:* $250\,\mu A/cm^2$ *(curve 1),* $600\,\mu A/cm^2$ *(curve 2) and* $1.2\,\mu A/cm^2$ *(curve 3). Inset: dependence* $(\alpha h\nu)^2 = f(h\nu)$ *of the* ZnO *layers with thicknesses in the range* $(120 \div 2300)nm$ *(current density of* $620\,\mu A/cm^2$ *.*

CuO

In Fig. 12 the absorption spectra of thin layers of CuO on glass substrate, obtained by thermal oxidation of the Cu layers at temperature of $500\,K$ in the air for $20\,\text{min}$, $100\,\text{min}$ and $180\,\text{min}$ are presented. As it can be seen, the absorption coefficient $\alpha(h\nu)$ for $h\nu < 2.3\,eV$ correlates with heat treatment time and is decreasing at increasing oxidation time. Absorption coefficient at $632.8\,nm$ is equal to $2.0\times10^4\,cm^{-1}$, and $2.3\times10^4\,cm^{-1}$ respectively for the treatment of $180\,\text{min}$, $100\,\text{min}$ and $20\,\text{min}$.

The spectral dependence of the absorption in the studied energy range is described by the function of the (13) type. The power factor $n = 2$ for the energies in the range of $2.1\,eV$ - $2.4\,eV$ and $n = 1/2$ for $h\nu > 2.5\,eV$. Direct band gap $293\,K$ does not depend on the oxidation time of copper layers (oxidation time lies in the range of $(20 \div 180)\text{min}$) and is equal to $2.33\,eV$. Optical band gap determined by linear extrapolation of the linear segment of the dependence $(\alpha h\nu)^{1/2} = f(h\nu)$ by $\alpha h\nu = 0$ for the layers heat-treated for $100\,\text{min}$, is equal to $1.72\,eV$ (inset in Fig. 12).

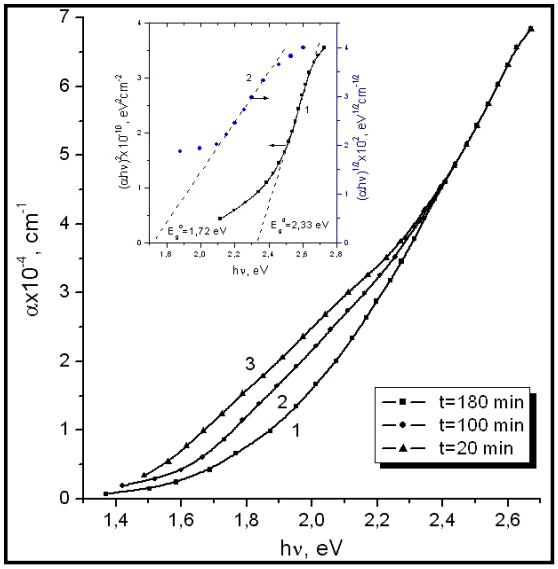

Fig. 12. Absorption spectra at 293 K for CuO thin layers heat-treated for 20, 100 and 180 minutes. Inset: $(\alpha h\nu)^2 = f(h\nu)$ *dependence (curve 1) and* $(\alpha h\nu)^{1/2} = f(h\nu)$ *(curve 2) of the CuO layers heat-treated for 1000 min.*

Cd_2O

Absorption spectra of thin layers of Cd_2O obtained on glass substrate by oxidation in air at 470 K of the ayers of Cd are shown in Fig. 13. As can be seen from the comparison of curves 1-3, the value of the absorption coefficient at given energy, and the spectral dependence of absorption coefficient is dependent on the oxidation process time. So, the absorption coefficient at 632.8 nm decreases from 1.9 × 10^4cm -1 down to $9.6\times10^3\,cm^{-1}$ when for the annealing time increases three times from $15\,\text{min}$ up to $45\,\text{min}$.

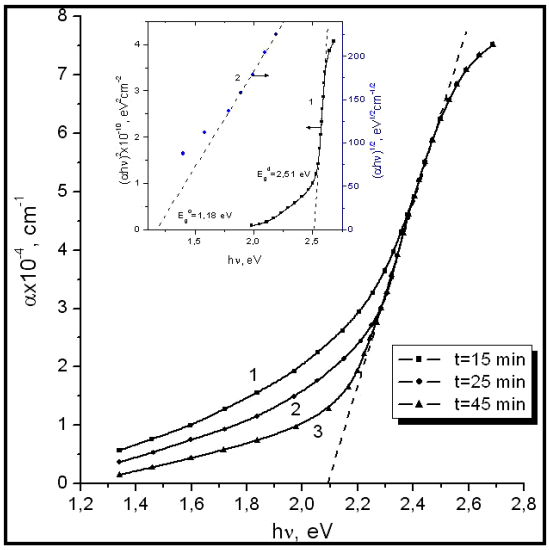

Fig. 13. Absorption spectra at 293 K for thin layers of Cd_2O *heat-treated for 15, 25 and 45 minutes. Inset:* $(\alpha h\nu)^2 = f(h\nu)$ *dependence (curve 1) and* $(\alpha h\nu)^{1/2} = f(h\nu)$ *(curve 2) of the* Cd_2O *layers at 293 K.*

At low energies $(1.6 \div 2.2)eV$, the spectral dependence $(\alpha h\nu)^{1/2} = f(h\nu)$ (inset to Fig.13, curve 2) is a segment of straight line. Optical band gap determined by extrapolation to $\alpha h\nu = 0$ of the segment of straight line is equal to $1.18eV$ at $T = 293K$. For $h\nu > 2.5eV$ direct transitions take place (inset Fig.13, curve 1). Direct band gap at $293K$ equals to $2.51eV$.

TiO_2/GaSe:Cu and TiO_2/InSe:Cu heterojunctions

Spectral characteristics of photocurrent for $TiO_2/GaSe:Cu$ and $TiO_2/InSe:Cu$ heterojunctions in which thin layers of TiO_2 were obtained by reactive evaporation in atmosphere of $Ar:O_2$ $(75:25)$ at different current densities in plasma, are shown in Figure 14. HJ photosensitivity is limited in both sides. Energy limits of photosensitivity are $1.00eV$, $1.80eV$ and $\sim 3.50eV$ for $InSe:Cu/TiO_2$ and $GaSe:Cu/TiO_2$. Edges on the low energy of the photosensitivity for investigated structures are determined by the absorption of light in $InSe$ and respectively in $GaSe$; edge towards high energy is caused by light absorption in TiO_2 layer (Figure 9).

Monotonous increase of the photosensitivity in energy range $1.5eV \le h\nu \le 3.0eV$ for HJ $TiO_2/InSe:Cu$, respectively in energy range $2.2eV \le h\nu \le 3.0eV$ for HJ $TiO_2/GaSe:Cu$ is in good correlation with formula (2). This serves as indicator of the presence of low concentrations of recombination states in $InSe:Cu$ and $GaSe:Cu$ layers; the states are localized at the interface of heterojunctions.

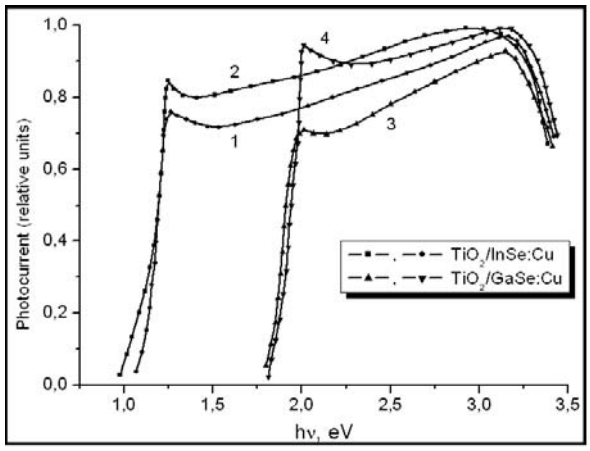

Fig. 14. Photocurrent spectral dependence for $TiO_2/InSe:Cu$ (curve 1, 2) and $TiO_2/GaSe:Cu$ (curve 3, 4) HJ at $293K$. The current density: $250\,\mu A/cm^2$ (curve 1), $500\,\mu A/cm^2$ (curve 3) and $750\,\mu A/cm^2$ (curve 2, 4).

As shown above, $InSe$ and $GaSe$ are semiconductors in which the band gap corresponds to indirect optical transitions. The absorption coefficient of light in a broad range of energies is less than $10^4 cm^{-1}$.

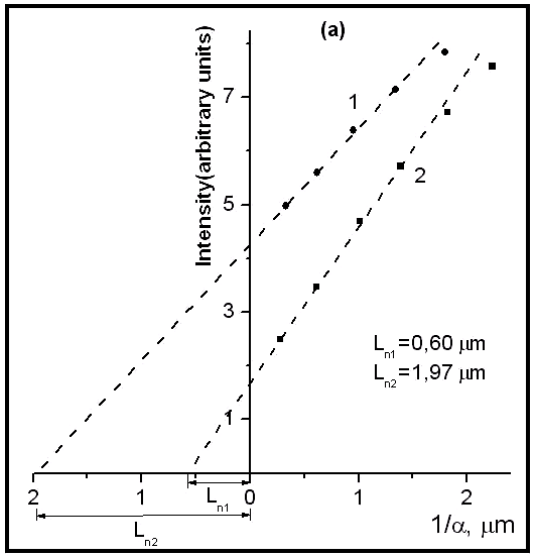

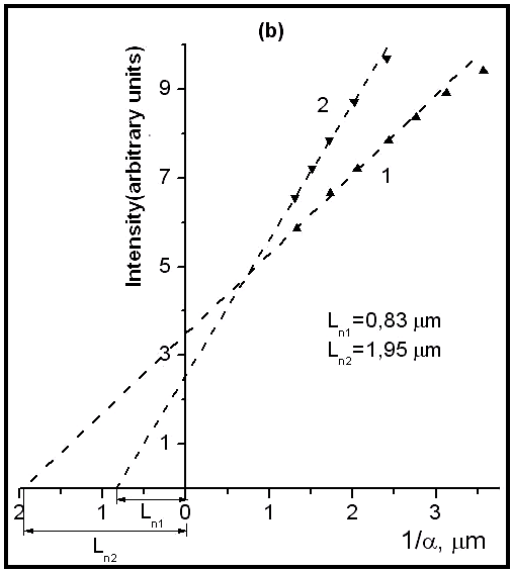

Fig. 15. The determination of mean free path of electrons in $InSe:Cu$, $GaSe:Cu$ layers from the interface of heterojunctions $InSe:Cu/TiO_2$ (a) $GaSe:Cu/TiO_2$ (b) at $293K$.

So, the inequalities $\alpha d_n << 1$, $d_n < L_p$ are satisfied and, if one considers that the recombination rate S_n is independent of the excitation intensity, by using (2) and (7) one obtains:

$$V_f = \frac{KT}{e}\frac{\alpha N_F}{\alpha L_p + 1}. \quad (14)$$

Varying $\alpha(h\nu)$ and adjusting the photon beam incident on the sample $\Delta N_F(h\nu)$ so that $V_F(h\nu)$ remains constant, and using (14) one obtains:

$$\Delta N_F(h\nu) = C\left(L_p + \frac{1}{\alpha}\right). \quad (15)$$

The dependencies of the variations of intensity of monochromatic light beam $\Delta N_F(h\nu)$ (in relative units) as function of $1/\alpha$ are show in Figure 15a and 15b n. Extrapolated linear segment of the dependence to the intersection with the $1/\alpha$ axis, determined the mean free path for minority charge carriers (electrons) in $InSe:Cu$ and $GaSe:Cu$ layers from the interface of heterojunctions $InSe:Cu/TiO_2$ (Figure 15a) and $GaSe:Cu/TiO_2$ (Figure 15b) as being equal to $0{,}6\,\mu m$, $1.97\,\mu m$ and $0.83\,\mu m$, $1.95\,\mu m$, respectively.

Heterojunctions In_2O_3/InSe:Cu

The band gap of undoped In_2O_3 layers at $T = 293\,K$ is equal to $E_g(0) = 3.63\,eV$ [42, 43]. Considering the optical band of In_2O_3 layers from $In_2O_3/InSe:Cu$ HJ at $T = 293\,K$ equal to $3.78\,eV$ one can conclude that the Fermi level is located deep in the conduction band at $\Delta E = E_g - E_g(0)$ - $0.15\,eV$.

The band gap coming from Burstein-Moss theory is given by the relationship [44]:

$$E_g = E_g(0) + \frac{\hbar^2}{2m^*}\left(3\pi^2 n\right)^{2/3} \quad (16)$$

where n is the concentration of electrons and m^* is the reduced mass of electrons and holes and is equal to $0.6\,m_0$ [45]. The result for the free charge carriers (electrons) concentration in In_2O_3 layers obtained by thermal oxidation of In layer in air , correlates well with the results given in paper [43]; in that paper, indium oxide was obtained by oxidation of the In layer in the O_2 containing ambient.

For $\Delta E = 0.15\,eV$, considering (16), one obtains the electron concentration in In_2O_3 layer equal to $6.9\times10^{19}\,cm^{-3}$.

In Figure 16a the spectral dependencies of photocurrent normalized to the number of incident photons on the sample per time unit for $In_2O_3/InSe:Cu$ HJ are shown. The low energy photosensitivity edge coincides with the edge of intrinsic absorption band in monocristalin samples of $InSe$. Therefore, it is assumed that the generation of non-equilibrium charge carriers takes place in $InSe$ layer from heterojunction's interface. Photosensitivity band edge at higher energies is determined by light absorption in In_2O_3 layer (Figure 7).

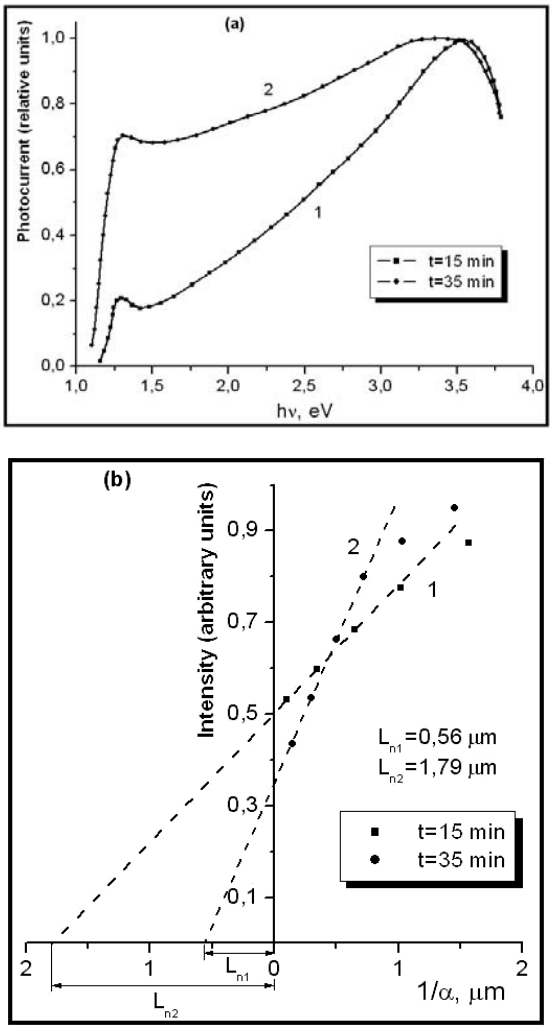

Fig. 16. (a) Spectral dependence of photocurrent of HJ $In_2O_3/InSe(0.02\%at.Cu)$ *at temperature* $293\,K$. *The duration of the oxidation of* In *layer:* $15\,\min$ *(curve 1) and* $35\,\min$ *(curve 2).* (b) Determination of the free path of electrons in the layer of $InSe:Cu$ from the interface of HJ $InSe(0.02\%at.Cu)/TiO_2$.

As can be seen in Figure 16a, the increase of the oxidation time of the In layer deposited onto the surface of $InSe$ layer leads to increase of the photosensitivity in the red spectral region, although the absolute maximum of photosensitivity is located at $\sim 3.5\,eV$.

Monotonically increasing of the photosensitivity of HJ $In_2O_3/InSe:Cu$ with energy in energies range from $1.5eV$ up to $3.4eV$ indicates that the recombination speed of minority charge carriers in the $InSe$ layer from HJ interface can be neglected.

The mean free path of electrons L_n in $InSe$ layer from the interface of the $In_2O_3/InSe$ HJ depends on the heat treatment time (Figure 16b). The increase of the In layer oxidation time from the $15\min$ up to $35\min$, results in mean free path of electrons is decreasing from $1.79\,\mu m$ down to $0.56\,\mu m$. It can be concluded that, during the oxidation process of metal layer (In), the diffusion of metal atoms in $InSe$ layer occurs and the creation of recombination centers, which consequently leads to decreasing the free path of minority charge carriers takes place.

Heterojunctions oxide semiconductor (In_2O_3, SnO_2, ZnO, Bi_2O_3, Cu_2O)/p-GaSe(Cu)

Semiconductor oxide (ITO, ZnO, Bi_2O_3, SnO_2 and Cu_2O) / $p-GaSe(Cu)$ HJ are photosensitive in the visible spectrum. In Figure 17a a spectral characteristic of the junction current to photon energy ratio as function of incident beam photon energy for $ITO/GaSe(Cu)$ at $T=293\,K$ HJ is presented. In the $(2.0\div\sim 3.2)eV$ range there is a continuous growth trend for the current, which indicates the relatively low concentration of surface states in the layer of $GaSe$ from HJ interface. In this spectral range, the absorption coefficient increases from $10^3\,cm^{-1}$ up to $\sim 10^5\,cm^{-1}$ [46]. Average thickness of $GaSe$ layer in which the non-equilibrium charge carriers are generated varies within $(0.1\div 10)\,\mu m$. For $h\nu > 3.2\,eV$ with the band-to-band transitions in the center of Brillouin zone, electronic transitions take place from the second valence sub-band to the conduction band.

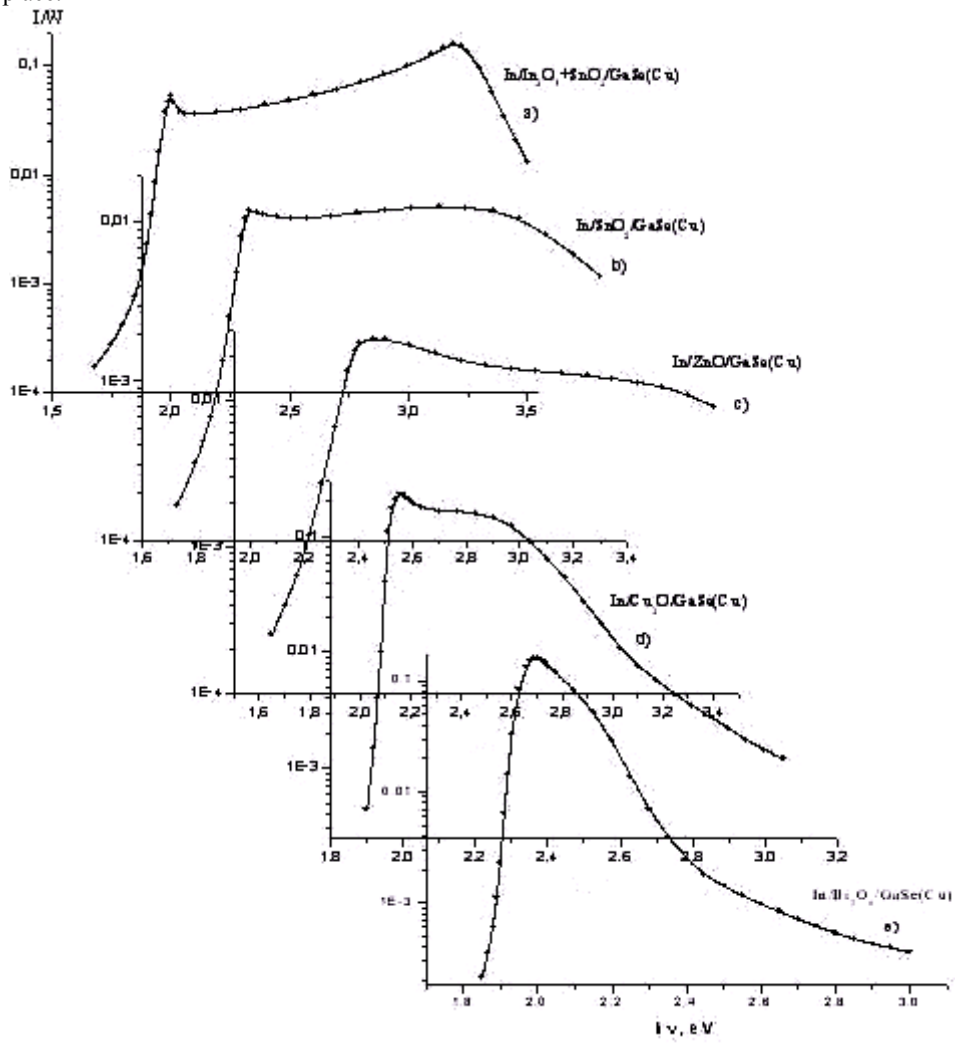

Fig. 17. Spectral dependence of photocurrent relative to the photon energy as function of photon energy for HJ (ITO, ZnO, Bi_2O_3, SnO_2 *and* Cu_2O) / $p-GaSe(Cu)$ *at temperature* $293\,K$.

These electronic transitions are determined by the absorption coefficients $\alpha >> 10^5 cm^{-1}$ and occurs in a layer of $GaSe$ having the average thickness $d << 0.1 \mu m$. Since in this spectral range the HJ photocurrent is decreasing rapidly with increasing photon energy, one can consider that in the layer of $GaSe(Cu)$ from HJ interface ($d << 0.1 \mu m$)low life-time surface states are present The recombination of non-equilibrium charge carriers through these surface states is more important than the recombination through energetic states from band gap.

The edge of photosensitivity band of $ITO/GaSe(Cu)$ HJ (Figure 17a) is located in the range of impurity photoconductivity ($h\nu \sim 1.65 eV$). In the spectral range $(1.65 \div 1.80) eV$ and is located also the absorption band of acceptor levels determined by Cu atoms [47].

A rapid increase of the quantum efficiency of light absorption by impurity levels are revealed in $SnO_2/p-GaSe(Cu)$ (Figure 17b) and $ZnO/p-GaSe(Cu)$ (Figure 17c) heterojunctions. Analogous to the $ITO/p-GaSe(Cu)$ heterojunctions, this growth is completed with a well pronounced peak at about $2.0 eV$ corresponding to the direct optical transitions in the center of Brillouin zone (Γ point). Monotonic decrease of quantum efficiency with increasing photon energy can serve as indicator of the presence of a gradient of surface states in the layer of $GaSe$ from interface of $SnO_2/p-GaSe(Cu)$ and $ZnO/p-GaSe(Cu)$ heterojunctions. The density of these energy states decreases when the distance from the interface in the $GaSe$ crystal increases. The range of photosensitivity of these heterojunctions is quite broad and covers the visible and near UV spectrum.

The mean free path of electrons in $GaSe$ layer from the interface of $In_2O_3/GaSe(Cu)$ and $SnO_2/GaSe(Cu)$ heterojunctions, resulted from Figure 18, is equal to $3.45 \mu m$ and $1.00 \mu m$ respectively.

The density of recombination states is higher in the $GaSe$ layer from the interface of $Cu_2O/p-GaSe(Cu)$ HJ, and especially in $Bi_2O_3/p-GaSe(Cu)$ HJ (Figure 17e and Figure 17d). It is assumed that during the annealing process heat treatment at temperature at $(600 \div 700) K$, the diffusion of Cu and Bi atoms in the $GaSe$ substrate occurs. Localized states in the $GaSe$ layer at the interface are generated facilitating the recombination of non-equilibrium charge carriers as well as low life-time surface states through which the charge carriers diffusing to the junction rapidly recombine.

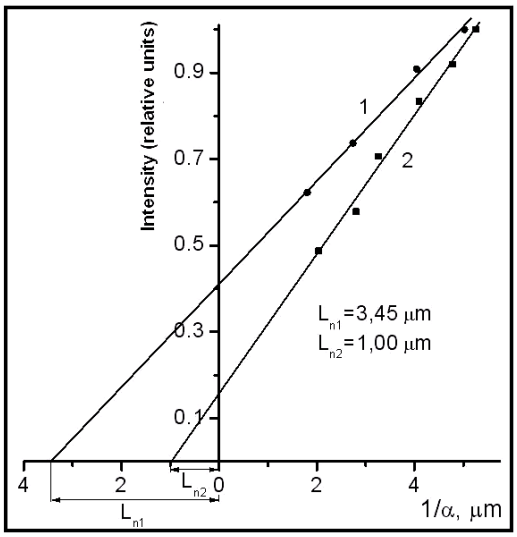

Fig. 18. Determination of length of free path for electrons in the $GaSe$ layer from interface of HJ $In_2O_3/GaSe(Cu)$ (curve 1) and $SnO_2/GaSe(Cu)$ (curve 2).

In Fig. 19 the spectral characteristic of the photoconductivity of $GaSe(Cu)$ monocrystalline layers (curve 2) and absorption spectrum of these layers (curve 1) are presented.

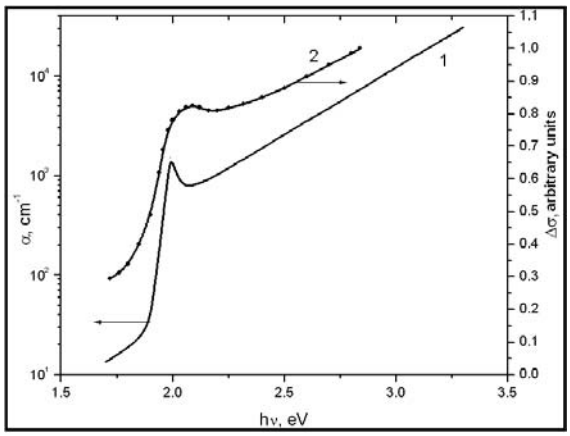

Fig. 19. Absorption coefficient spectral dependence of $GaSe(0.05\%at.Cu)$ monocrystalline layers (curve 1) and spectral distribution of photoconductivity for $GaSe(0.05\%at.Cu)$ crystals (curve 2).

As can be seen in these presentations, at energies $h\nu > 2.1 eV$ photoconductivity of $GaSe(Cu)$ monocrystalline layers increases together with absorption coefficient α. Considering that that relatively small thickness of $GaSe$ layer ($d \approx 12 \mu m$) used to manufacture heterojunctions satisfy the condition of total absorption of photons in the sample ($\alpha d >> 1$), one

should consider that photoconductivity is proportional to the total number of absorbed photons A:

$$\Delta\sigma = A \cdot \tau, \tag{17}$$

where τ is the life-time of non-equilibrium charge carriers. At low intensities of illumination the life-time can be assumed to be constant .

Linear growth of the absorption coefficient and of the photoconductivity deep inside of fundamental absorption band serve as direct evidence about the relative low value of the rate of recombination of non-equilibrium charge carriers through the surface states in $GaSe(Cu)$ crystals.

Illuminating the $Bi_2O_3/GaSe(Cu)$ structure through Bi_2O_3 layer with photons $h\nu > 1.7eV$, the separation of non-equilibrium charge carriers occurs at junction. The photocurrent I/W normalized to the number of incident photons reaches its maximum value at energies corresponding to the absorption band of Cu impurities $h\nu \approx 1.88eV$ and it has a decreasing trend with increasing photon energy. Since the edge of absorption band of the $GaAs(Cu)$ layer coincides with the edge of the photocurrent through the junction ($I(h\nu)$) one can consider that the non-equilibrium charge carriers are generated in $GaSe(Cu)$ layer from $Bi_2O_3/GaSe(Cu)$ junction. Slow decrease of photocurrent with the increase of the absorption coefficient α indicates the presence of surface states with small life-time (high recombination rate). Such states are probably created by atoms of Bi_2O_3 layer that generates new valence bounds with Se atoms from the surface of $Se-Ga-Ga-Se$ layered structure.

At forward biases of $ZnO/GaSe(Cu)$ HJ at voltages higher than the build-in voltage, a "flattening" of energy bands occurs. In this case the photocurrent in circuit is determined by the speed of generation of non-equilibrium charge carriers and by recombination process through recombination levels situated inside band gap and also by recombination process on surface states characterized by recombination rate S. The photocurrent intensity is given by [47]:

$$I_{fc} \sim \frac{(1-R)\eta N_f\left(1-e^{-\alpha d}\right)}{1+Re^{-\alpha d}} \times \times\left[1+\frac{S}{D_n}L_n\frac{cth\frac{d}{2L}-\alpha L cth\frac{\alpha d}{2}}{1-\alpha^2L^2}\right], \tag{18}$$

where D_n is the diffusion coefficient of the minority charge carriers in the $GaSe$ layer at the junction interface; d is the $GaSe$ layer thickness.

For $d >> L_n$ and $d >> 1/\alpha$ from (18) one obtains:

$$I_{fc} \sim 1+\frac{S}{D}\frac{L}{1+\alpha L_n}. \tag{19}$$

In the domain of high absorption coefficients ($\alpha >> 1/L_n$), the photocurrent linearly depends on the value of the inverse of the absorption coefficient

$$I_{fc} \sim 1+\frac{S}{D}\frac{1}{\alpha}. \tag{20}$$

In Figure 20 the dependence of photocurrent normalized to incident photons number vs the inverse value of the absorption coefficient for the $ZnO/GaSe$ structure at forward bias at $5V$ is shown. The D/S determined by the interception on the axis $1/\alpha$, is equal to $6.65\mu m$.

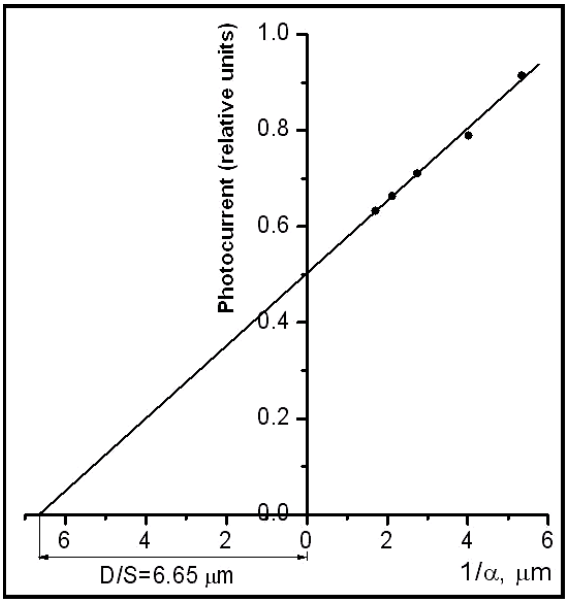

Fig. 20. Dependence of photocurrent normalized at incident photons number on the inverse of absorption coefficient for the ZnO/GaSe structure at forward bias.

The photocurrent vs illumination (*J-F*) dependencies for HJ reverse biased $U = 5V$ were measured for structures based on $GaSe:Cu$. The incident light had the wavelength in the range of $(520 \div 610)nm$ (selected with a set of optical filters from the spectrum of the lamp with tungsten filament at $2850K$). Heterojunctions based on $InSe:Cu$ were illuminated with a light beam having its wavelength in the range of $(0.4 \div 1.1\mu m)$ selected from the same source. As it comes from the presented $J(F)$ plot, in the range of illumination from $0.1lux$ up to $1000lux$ the dependencies are linear. The current sensitivity is $\sim 1\mu A/lx$.

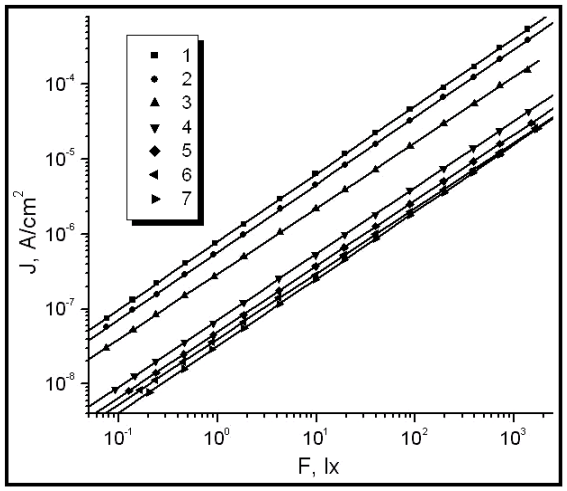

Fig. 21. Dependence of short circuit current on illumination of heterojunctions: $In_2O_3/GaSe:Cu$ *(1);* $In_2O_3:Sn/GaSe:Cu$ *(2);* $TiO_2/GaSe:Cu$ *(3),* $ZnO/GaSe:Cu$ *(4)* $CuO/GaSe:Cu$ *(5);* $Cd_2O/GaSe:Cu$ *(6);* $Bi_2O_3/GaSe:Cu$ *(7).*

To determine the mechanism of charge carriers transport through the junction current -voltage (IU) characteristics were measured at direct (Figure 22a) and reverse bias (Figure 22b) of HJ. At low voltages ($U < 0.25V$) IU characteristics for (CdO, TiO_2, ZnO)$/GaSe:Cu$ HJ is practically exponential and are described by [48]:

$$J = J_0 \cdot \left[\exp\cdot\left(qV/nKT\right) - 1\right] \qquad (21)$$

where J_0 - density of current determined by minority charge carriers; q - elementary charge, K - Boltzmann constant and T - absolute temperature. The diode quality factor (n) of the studied structures is $(\sim 1.5 \div 1.6)$. The value of n greater than unity indicate that, along with diffusion current

$$J_d = \left(\frac{qD_p p_{n0}}{L_p} + \frac{qD_n n_{p0}}{L_n}\right)\left(\exp\frac{qV}{KT} - 1\right) \qquad (22)$$

in the junction there is a current J_r determined by intense recombination of minority charge carriers (2).

IU characteristics at forward biasing $U > 0.3V$ is quasi - linear determined by voltage drop on bulk material ($GaSe:Cu$) outside the junction.

In Figure 22b, the IU dependencies are presented for at reverse bias of (CdO, TiO_2, ZnO)$/GaSe:Cu$ heterojunctions. At voltages $U < 1V$, the IU characteristics are described well by a power function of $J \sim U^k$ type, where the power factor k has the value of 0.8 for the $TiO_2/GaSe:Cu$, 0.88 for $Cd_2O/GaSe:Cu$ and 0.9 for $ZnO/GaSe:Cu$ HJ. At voltages $U > 1V$, the power factor increases up to $(2.9 \div 3.9)$, which is in good agreement with the space charge limited current [49].

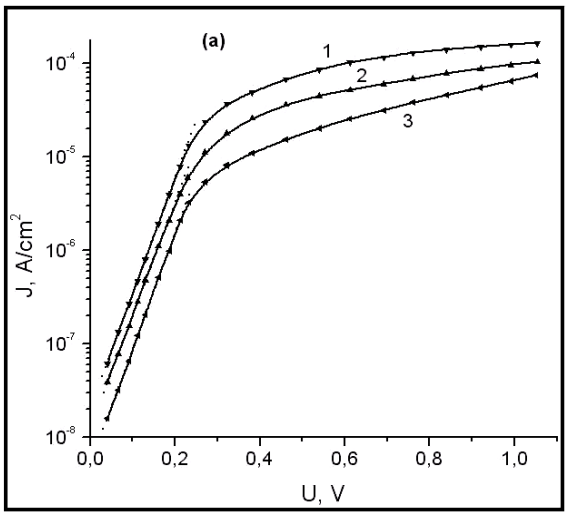

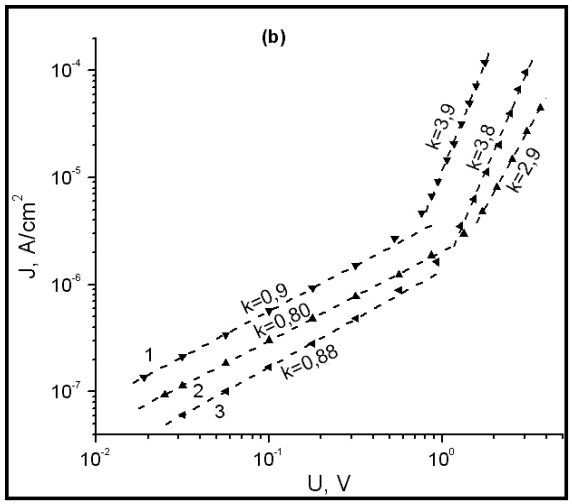

Fig. 22. Current-voltage characteristic at the temperature $293K$ *for structures* $ZnO/GaSe:Cu$ *(1),* $TiO_2/GaSe:Cu$ *(2) and* $Cd_2O/GaSe:Cu$ *(3) to direct (a) and reverse polarization (b).*

From the analysis of: absorption spectra of $GaSe$, $InSe$ crystal and of In_2O_3 thin layers, spectral characteristics of photosensitivity of $In_2O_3/InSe:Cu$ and $In_2O_3/GaSe:Cu$ HJ, and knowing electronic affinity of materials, being equal to $3.70eV$ (In_2O_3), $4.55eV$ ($InSe$) and $3.8eV$ ($GaSe$) the energy diagrams of the

junction $In_2O_3/GaSe$ and $In_2O_3/InSe$ (Fig. 23) were approximated.

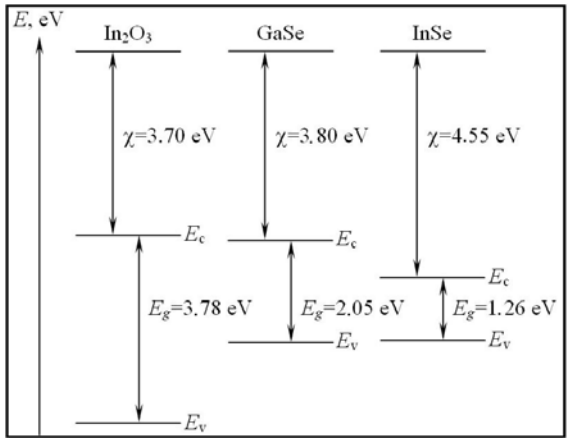

Fig. 23. Energy diagrams of the junction $In_2O_3/GaSe$ *and* $In_2O_3/InSe$.

3. Conclusions

There the absorption spectra of $GaSe$, $InSe$ monocristalin layers at $293K$ and $78K$ were analyzed. The exciton characteristics and characteristic energies of electronic bands structure were determined.

The character of optical transitions and the band gap of oxides of metals (In, Sn, Ti, Bi, Zn, Cu and Cd) layers were determined.

The photosensitivity bands and charge carriers transport mechanism for $GaSe$, $InSe$ semiconductors and metals' oxides of In, Sn, Ti, Bi, Zn, Cu and Cd were determined.

As it came from the analysis of absorption and photosensitivity spectra the value of diffusion mean path of minority charge carriers in $InSe$ and $GaSe$ layer from interface of $InSe:Cu/TiO_2$ and $GaSe:Cu/TiO_2$ HJ at $293K$ and $78K$ as being equal to $0.60\mu m$, $1.97\mu m$ and $0.83\mu m$, $1.95\mu m$, respectively was determined.

It was established that mean free diffusion path is decreasing with increase of In layer oxidation time deposited on the surface of $GaSe$ and $InSe$ monocristalin films.

The ratio of recombination rate of non/equilibrium charge carriers through surface states and diffusion coefficient in $GaSe$ layer from interface of HJ $ZnO/GaSe:Cu$ was determined: $6.65\mu m$.

References

[1] B. L. Evans Optical and Electrical properties of layer compounds. Edit by P. A. Lee-Bostov; Dordrecht, 1976.
[2] M. S. Brodin, I. V. Blonskii, Excitonnîe protessî v sloistîh cristallah. Kiev, Naukova Dumka, 1986, p. 251.
[3] Chang-Dae Kim, Ki-Wan Jang, Yong-Ill Lee, Solid State Commun. **130,** 701 (2004).
[4] M. Grandolfo, F. Somma, P. Vecchia, Phys. Rev. B **5,** 428 (1972).
[5] B. Gürbulak, Solid State Commun. **109,** 665 (1999).
[6] J. Martinez-Pastor, A. Segura, J. L. Valdés, A. Chevy, J. Appl. Phys. **62** (1987) 1477.
[7] A. G. Kyazim-Zade, R. N. Merkhtieva, A. A. Akhmedov, Semicond. **25,** 840 (1992).
[8] A. Castellano, Appl. Phys. Lett. **48**(4), 298 (1986).
[9] S. Shigetomi, T. Ikari, J. Appl. Phys. **88**(3) (2000) 1520.
[10] Z. D. Kovalyuk, V. M. Katerynchuk, A. I. Savchuk, O. M. Sydor, Mater. Science Eng. B **109,** 252 (2004).
[11] Z. D. Kovalyuk, V. M. Katerynchuk, O. M. Sydor, J. Optoelectron. Adv. Mater. **7**(2), 903 (2005).
[12] O. Lang, Y. Tomm, R. Schlaf, C. Petterkofer, W. J. Jaegermann, Appl. Phys **75**(12), 7814 (1994).
[13] V. L. Bakumenko, Z. D. Kovalyuk, L. N. Kurbatov, V. G. Tagyev, V. F. Chisko, Semiconductors (rus) **14**(6) (1980) 1115.
[14] Z. D. Kovalyuk, P. G. Lytovchenko, O. A. Politanskaia, O. N. Sidor, V. M. Katerynchuk, V. F. Lastovechky, O. P. Litovchenko, V. K. Dubovoy, L. A. Polivtsev, Semiconductors (rus) **41**(5), 570 (2007).
[15] Kovalyuk M. Z., Tovarnitsky M. V., J. Optoelectron. Adv. Mater. **5** (4) (2003) 853.
[16] V. P.Savchyn, V. B. Kytsai, Thin Solid Films **361-362,** 123 (2000).
[17] A. P. Bahtinov, Z. D. Kovalyuk, O. N. Sydor, V. N. Katerynchuk, O. S.Lytvin, Phys. Sol. Stat. (rus) **49**(8), 1497 (2007).
[18] E. H. Putley, Phys. Stat. Sol. (b),**6,** 571 (1964),.
[19] T. S. Moss, G. J. Burrell, B. Ellis, Semiconductor optoelectronics. - New York: Halsted Press Division, Wiley, 1973. - p. 17.
[20] Y. Laaziz, A. Bennouna, N. Chahboun, et al. Thin Solid Films, **372** (1-2), 149 (2000).
[21] E. D. Stokes, T. L. Chu, Appl. Phys. Lett., **30**(8), 425 (1977).
[22] Y. Marfaing, Handbook on semiconductors. - Edit. M. Balkan Sky: Elsevier, 1994. - 758 p.
[23] J. J. Loferski, J. Appl. Phys. **27**(7), 777 (1956).
[24] G. Hass, L. F. Drummeter, M. J. Schach, Opt. Soc. Am., **49**(9), 918 (1959).
[25] L. Z. Kriksunov, Handbook on infrared techniques Moskva Sov Radio 1978, p. 400 (in Russ).

[26] L. Z. Kriksunov Handbook on infrared techniques Moskva Sov Radio 1978, p . 120 (in Russian).
[27] Y. P. Varshni, Physica, **34**(1), 149 (1967).
[28] C.-D. Kim, K.-W. Jang, Y.-I. Lee, Solid State Communications, **130**(10), 701 (2004).
[29] Singleton J. Band Theory and Electronic Properties of Solids. - Oxford: University Press, 2001. - 240 p.
[30] Excitons. Contemporary problems of condensed matter science. Pajba E.I. I Sterdja M.D. Moskva Nauka 1985 p. 616 (in Russian).
[31] M. S. Brodin, I. V. Blonskii Excitonic process in crystals – Kiev Naukova dumka, 1986,- p 256 (in Russian).
[32] B. S. Razbirin, A. N. Staruhin, E. M. Gamart et all Pisma v JETF, **27**(6), 341 (1978).
[33] R. J. Elliott, Phys Rev. **108,** 1384 (1957).
[34] V. P. Gribkovskii, Theory of light absorption p/pr – Minsk. Nauka I tehnica, 1975, p 463 (in Russian).
[35] A. Seyhan, O. Karabulut, B. G. Akinoğlu, et al. Cryst. Res. Technol., **40**(9), 893 (2005).
[36] R. L. Toullec, N. Piccioli, J. C. Chervin, Phys. Rev. B**22**(12), 6162 (1980).
[37] V. Capozzi, Physical Review B**28**(8), 4620 (1983).
[38] Physical and chemical properties of semiconductors – Z. S. Medvedeva, O. N. Kalashnik, Ia. A. Kalashnikov, - Moskva, Nauka, 1979, - p 339 (in Russian).
[39] C. D. Lokhande, A. U. Ubale, P. S. Patil, Thin Solid Films, **302**(1-2), 1 (1997).
[40] Y. P. Varshni, Phys. Stat. Sol. (b), **19**(2), 459 (1967).
[41] W. A. Badawy, R. S. Momtaz, E. M. Elgiar, Phys. Stat. Sol. (a), **118**(1), 197 (1990).
[42] O. Lang, C. Pettenkofer, J. F. Sánchez-Royo, et al. J. Appl. Phys., **86**(10), 5687 (1999).
[43] H. Öfner, Y. Shapira, F. P. Netzer, J. Appl. Phys., **76**(2), 1196 (1994).
[44] K. Seeger Semiconductor physics. - New York: Springer-Verlag, Wien, 1973. - 615 p.
[45] I. Hamberg, C. G. Granqvist, J. Appl. Phys. **60**(11), R123 (1986).
[46] E. Cuculescu, I. Evtodiev, M. Caraman, E-MRS IUMRS ICEM 2006 Spring Meeting, Nice, France, May 29 - June 2, 2006, Book of abstracts.
[47] V. K. Subashiev FTT **6**, 1956 (1964).
[48] S. M. Sze Physics of Semiconductor Devices. – Moscow: Mir, **2**, 456 (1984).
[49] M. A. Lampert, Mark P. Current injection in solids. - New York: Academic Press, 1970. - 351 p.

*Corresponding author: asdafinei@yahoo.com